Ground-state correlation energy of beryllium dimer by the Bethe-Salpeter equation

Jing Li,[1, 2, 3] Ivan Duchemin,[1, 3] Xavier Blase,[1, 2] and Valerio Olevano[1, 2, 4]

[1] *Université Grenoble Alpes, 38000 Grenoble, France*
[2] *CNRS, Institut Néel, 38042 Grenoble, France*
[3] *CEA, INAC-MEM L_Sim, 38054 Grenoble, France*
[4] *European Theoretical Spectroscopy Facility (ETSF)*
(Dated: December 4, 2018)

The interatomic potential of the beryllium dimer Be_2 has been since the '30s both an experimental and theoretical challenge. The calculation of the ground-state correlation energy of Be_2 along its dissociation path is a difficult problem for theory. We present *ab initio* many-body perturbation theory calculations of the Be_2 interatomic potential using the *GW* approximation and the Bethe-Salpeter equation (BSE). The ground-state correlation energy is calculated by the trace formula with checks against the adiabatic-connection fluctuation-dissipation theorem formula. We show that inclusion of *GW* corrections already improves even at the level of the random-phase approximation. At the level of BSE on top of *GW*, our calculation is surprisingly in agreement with the most accurate theories and the experiment. It even reproduces an experimentally observed flattening due to a correlations delicate balance from a competition between covalent and van der Waals bonding.

Introduction. The beryllium dimer Be_2 has a long scientific history, with hundreds of experimental and theoretical investigations [1, 2]. The first synthesis of Be_2 was attempted in the '30s with no success [3, 4], while Hartree-Fock (HF) or other theoretical modelling [5, 6] found a repulsive ground-state, leading to the conclusion that Be_2 does not exist. Later studies [2, 7] pointed to a possible van der Waals binding with a shallow minimum at large (~ 5 Å) distance, while others yielded a double short and long-range minimum [2, 8]. Be_2 remained elusive till the '70s [9], and only in the '80s first rotovibrational spectra were measured [10] and reliable calculations [11] were made, both pointing to a single short-bond minimum at ~ 2.5 Å. Today we have very accurate experiments [1] and calculations [12] for the Be_2 interatomic potential. Nevertheless, Be_2 remains a severe workbench to check many-body theories, and this is the purpose of this work.

The description of the correlation energy of molecular dimers along their dissociation path is a theoretical challenge [13, 14]. Full configuration interaction (CI) [14] is the only accurate method [2, 12] providing results in very good agreement with the experiment, though is limited to very small molecules. Quantum Monte Carlo (QMC) [13, 15–17], both variational (VMC) and diffusion (DMC) are also valid alternatives, and DMC is even exact in systems where the ground-state wavefunction does not present nodes, but they can be also very cumbersome. Density-functional theory (DFT) [13] is in principle exact to calculate ground-state energies, but standard approximations, like the local-density (LDA) and generalized-gradient (GGA), have shown their limits on dimers binding energies and lengths [18], in particular in the dissociation limit. Time-dependent density-functional theory (TDDFT) [19, 20] in the adiabatic-connection fluctuation-dissipation theorem (ACFDT) formalism [21, 22] has in the recent years

been considered as one promising approach to improve over approximated DFT [18, 23–25]. It anyway relies on TDDFT approximations for the polarizability χ, such as the random-phase approximation (RPA), the adiabatic LDA (ALDA or TDLDA), or beyond. Nevertheless, the interatomic potential of Be_2 continues to be a problem also for TDDFT ACFDT, both in RPA [26] and also more advanced approximations [25, 27].

In this work, we calculate the Be_2 interatomic potential in the framework of *ab initio* many-body perturbation theory using the *GW* approximation [28] and the Bethe-Salpeter equation (BSE) [13, 29, 30]. The ground-state correlation energy is calculated by the trace formula (TF) [31, 32]

$$E_0^c = \frac{1}{2} \left[\sum_{i>0} \Omega_i - \text{Tr}(A) \right] \tag{1}$$

where Ω_i are the positive eigenvalues of the full, i.e. beyond Tamm-Dancoff approximation, BSE equation, and A is the only-resonant part of the BSE excitonic Hamiltonian. This formula was introduced by Sawada to calculate the correlation energy of the electron gas [33] as an alternative to the Gell-Mann & Brückner integration along the adiabatic connection on the interaction switch-on λ parameter formula [34]. The two were later shown to be equivalent both in RPA on the electron gas [35, 36] and in TDDFT ACFDT [37]. We confirm this equivalence, at least at the RPA level, by also evaluating the correlation energy via the TDDFT ACFDT formula [18, 21, 22]

$$E_0^c = \frac{1}{2\pi} \int du dr dr' \left[\ln\left(1 - \frac{\chi^0(r, r', iu)}{|r - r'|} \right) + \frac{\chi^0(r, r', iu)}{|r - r'|} \right]$$

where $\chi^0(r, r', iu)$ is the Kohn-Sham polarizability along the positive imaginary frequency axis $\omega = iu$, $u > 0$. Our results show that *GW* corrections introduce important improvements already at the level of RPA. The interatomic potential we obtain at the level of BSE on top of

GW is surprisingly in agreement with the most accurate calculations and the experiment. *GW*+BSE correlations seem even able to describe the unusual shape of the experimental [1] interatomic potential, a flattening of the Morse potential in the range [6,9] Bohr ($\sim$[3,4.5] Å) towards an expanded Morse potential which better fits the experimental vibrational spectrum [1].

The solution of the historical problem represented by the paradigmatic Be_2 interatomic potential, shows that the use of Eq. (1) in the BSE framework can reveal an accurate methodology to calculate the ground-state energy and stability of atoms and molecules, solids, and even nuclei, with an important advance in all these fields.

Theory. Eq. (1) was previously derived by different ways [33, 36, 37]. We here present a modification of the Thouless derivation [31, 38] which extends its validity to starting points different from HF towards DFT or *GW*, and to kernels beyond RPA towards BSE or TDDFT kernels. We start from the Bethe-Salpeter equation,

$$L = L^0 + L^0 \Xi L,$$

where L is the two-particle correlation function, $L^0 = GG$ with G the one-particle Green function, and Ξ the two-particle interaction, which is an exact equation to calculate the excitation spectrum. By knowing the exact Ξ and L^0 (so G), the BSE can be solved for L whose poles $\Omega_\lambda = E_\lambda - E_0$ and their associated residuals provide the neutral excitation energies and oscillator strengths. In practice approximations are unavoidable. We consider a quite general case of an approximated, e.g. HF, *GW* or DFT, electronic structure with real energies ϵ_i and orthonormal wavefunctions $\phi_i(r)$ used to build G and L^0, and an approximated static kernel, e.g. the TDH $i\Xi_{ijkl} = w_{iljk}$ (with w the bare Coulomb interaction), or the TDHF $i\Xi_{ijkl} = w_{iljk} - w_{ilkj}$, or the *GW*+BSE $i\Xi_{ijkl} = w_{iljk} - W_{ilkj}$ (with W the screened Coulomb interaction), or even the TDLDA. Under these conditions the Bethe-Salpeter equation can be reduced to the well known [13, 31, 39–41] RPA equation

$$\begin{pmatrix} A & B \\ B^* & A^* \end{pmatrix} \begin{pmatrix} X^\lambda \\ Y^\lambda \end{pmatrix} = \Omega_\lambda \begin{pmatrix} 1 & 0 \\ 0 & -1 \end{pmatrix} \begin{pmatrix} X^\lambda \\ Y^\lambda \end{pmatrix}, \quad (2)$$

with the Hermitian $A_{tt'} = A_{php'h'} = (\epsilon_p - \epsilon_h)\delta_{pp'}\delta_{hh'} + i\Xi_{php'h'}$ and the symmetric $B_{tt'} = B_{php'h'} = -i\Xi_{pp'hh'}$ matrices indexed by particle-hole transition indices $t = \{ph\}$ from an occupied h to an empty p state, $\hat{c}_p^\dagger \hat{c}_h$, on the orthonormal basis set $\phi_i(r)$. Eq. (2) provides a full spectrum of excitations $|\Psi_\lambda\rangle$, both excitation energies $\Omega_\lambda = E_\lambda - E_0$ (with respect to the ground state energy E_0) and eigenvectors $(X^\lambda \, Y^\lambda)$, which constitutes an approximation to the exact one. We now introduce *boson* [39] transition operators $\hat{C}_t$ replacing the *ph* operator bilinears, $\hat{c}_p^\dagger \hat{c}_h \to \hat{C}_t^\dagger$, i.e. fulfilling exact boson canonical commutation relations, $[\hat{C}_t, \hat{C}_{t'}] = 0, [\hat{C}^\dagger_t, \hat{C}_{t'}^\dagger] = 0, [\hat{C}_t, \hat{C}_{t'}^\dagger] = \delta_{tt'}$. This is not the case for the fermion

bilinears, $[\hat{c}_p \hat{c}_h^\dagger, \hat{c}_p^\dagger \hat{c}_h] \neq \delta_{pp'}\delta_{hh'}$. So that the ones can be seen as an approximation of the others. We now express the full many-body Hamiltonian $\hat{H}$ in terms of the boson operators under the condition to get, by construction, the same excitation spectrum of Eq. (2). This is granted if [39]

$$\langle \Psi_0 | [\hat{C}_t, [\hat{H}, \hat{C}_{t'}^\dagger]] | \Psi_0 \rangle = A_{tt'},$$
$$\langle \Psi_0 | [\hat{C}_t, [\hat{H}, \hat{C}_{t'}]] | \Psi_0 \rangle = -B_{tt'}.$$

Up to quadratic terms only [42] the Hamiltonian writes

$$\hat{H} = E_0^0 + \sum_{tt'} A_{tt'} \hat{C}_t^\dagger \hat{C}_{t'} + \frac{1}{2} \sum_{tt'} [B_{tt'} \hat{C}_t^\dagger \hat{C}_{t'}^\dagger + B_{tt'}^* \hat{C}_t \hat{C}_{t'}],$$

where the constant E_0^0 is approximated by the expectation value of the Hamiltonian, $E_0^0 = \langle \Phi_0 | \hat{H} | \Phi_0 \rangle$, over the 0-order ground-state Slater determinant Φ_0 constructed with the occupied wavefunctions $\phi_h(r)$ [43]. For HF orbitals $\phi^{\mathrm{HF}}(r)$, the constant is the HF ground-state energy $E_0^0 = E_0^{\mathrm{HF}}$, whereas for DFT is the kinetic, external, Hartree and exchange operators evaluated on the Kohn-Sham wavefunctions, $E_0^0 = E^{\mathrm{DFT}} - E_{\mathrm{xc}} + E_{\mathrm{EXX}}$. The Hamiltonian can be recast into a matrix form,

$$\hat{H} = E_0^0 - \frac{1}{2}\mathrm{Tr}(A) + \frac{1}{2} \left(\hat{C}^\dagger \ \hat{C} \right) \begin{pmatrix} A & B \\ B^* & A^* \end{pmatrix} \begin{pmatrix} \hat{C} \\ \hat{C}^\dagger \end{pmatrix},$$

and the solutions $(X^\lambda \, Y^\lambda)$ to Eq. (2), subject to the orthonormality condition $\sum_t (X_t^{\lambda*} X_t^{\lambda'} - Y_t^{\lambda*} Y_t^{\lambda'}) = \delta_{\lambda\lambda'}$, allows to define new boson operators $\hat{Q}_\lambda$ by a Bogoliubov transformation of the $\hat{C}_t$,

$$\hat{Q}_\lambda^\dagger = \sum_t (X_t^\lambda \hat{C}_t^\dagger - Y_t^\lambda \hat{C}_t),$$

which diagonalizes the Hamiltonian

$$\hat{H} = E_0^0 - \frac{1}{2}\mathrm{Tr}(A) + \frac{1}{2}\sum_\lambda \Omega_\lambda + \sum_\lambda \Omega_\lambda \hat{Q}_\lambda^\dagger \hat{Q}_\lambda. \quad (3)$$

The operators $\hat{Q}_\lambda$ act on the (approximated) ground $|\Psi_0\rangle$ and excited $|\Psi_\lambda\rangle$ states, $\hat{Q}_\lambda^\dagger |\Psi_0\rangle = |\Psi_\lambda\rangle$, $\hat{Q}_\lambda |\Psi_0\rangle = 0$, and the expectation value of the Hamiltonian Eq. (3) over the excited states $|\Psi_\lambda\rangle$ provides by construction the excitation energies Ω_λ with respect to the ground state. Finally, the expectation value of the Hamiltonian Eq. (3) over $|\Psi_0\rangle$ provides the total energy of the ground state *including correlation* (within stated approximations),

$$E_0 = E_0^0 + \frac{1}{2}\sum_\lambda \Omega_\lambda - \frac{1}{2}\mathrm{Tr}(A). \quad (4)$$

Thus, for a starting HF electronic structure, the last two terms beyond the constant $E_0^0 = E_0^{\mathrm{HF}}$ in Eq. (4) provide the correlation energy Eq. (1), alternatively recast

$$E_0^{\mathrm{corr}} = \frac{1}{2}\sum_\lambda (\Omega_\lambda - \Omega_\lambda^{\mathrm{TDA}}), \quad (5)$$

or also

$$E_0^{\text{corr}} = -\sum_\lambda \Omega_\lambda \sum_t |Y_t^\lambda|^2, \qquad (6)$$

where $\Omega_\lambda^{\text{TDA}}$ are the eigenvalues of Eq. (2) in the Tamm-Dancoff approximation (TDA), i.e. taking $B = 0$. Eqs. (5) and (6) more clearly show that the ground state correlation energy arises only beyond the TDA approximation and from terms in B and Y. The TDA is only able to introduce correlations in the excited states.

To resume, Eq. (4) is an expression for the ground-state total energy E_0 *including correlation at the same level of approximation* (e.g. RPA or TDHF, GW+BSE, etc.) taken for the A and B matrices, and of the associated excitation spectrum Ω_λ. In contrast to the ACFDT formalism, which provides an in principle exact formula for correlations within TDDFT, Eq. (4) is since the beginning only an approximated expression, relying on the validity of the boson approximation between operators, $\hat{C}_t \simeq \hat{c}_p^\dagger \hat{c}_h$, and of the killing condition on the 0-order Slater determinant ground-state, $\hat{C}_t |\Phi_0\rangle \simeq 0$. However for both formulas the most critical is the approximation on the kernel (RPA, TDLDA, GW+BSE) and on the starting electronic structure (LDA, GGA, HF, GW, etc.) Comparing the merits of the various approximations is still in its infancy for atoms and molecules [44, 45].

In order to provide the best comparison with previous literature and ACFDT results, we use the same large cc-pV5Z Gaussian basis set [46] adopted in Ref. [27], together with the auxiliary cc-pV5Z-RI basis set [47] in our Coulomb-fitting resolution-of-identity approach. Input Kohn-Sham or Hartree-Fock eigenstates were calculated by the NWChem [48] package, whereas many-body calculations were performed with the Fiesta [49, 50] code. For improved accuracy [49, 51] we performed evGW calculations, namely partially self-consistent GW on the eigenvalues, for all 4 occupied and 14 empty states.

Results. In Fig. 1 we present the interatomic potential of Be$_2$ as derived from recent accurate experimental rotovibrational spectra [1], and from the most accurate configuration interaction (CI) calculation [12] which is in good agreement with the experiment. We then present theoretical curves we calculated at the level of the direct RPA approximation on top of DFT in the PBE [52] approximation (RPA@PBE) by the TF [Eq. (4) or equivalently, which has been checked numerically, Eq. (6)], and by the ACFDT formulas. They are in perfect agreement. We can compare our RPA@PBE curves with those calculated by Refs. [26, 27] with the ACFDT formula. Although we used exactly the same calculation parameters reported in Ref. [27], our result differs from theirs, in particular on the binding energy, due to the basis set superposition error they mention and remove by counterpoise. We preferred not to use the counterpoise method following some works [53, 54] which found it less correct in the case of systems where van der Waals interaction
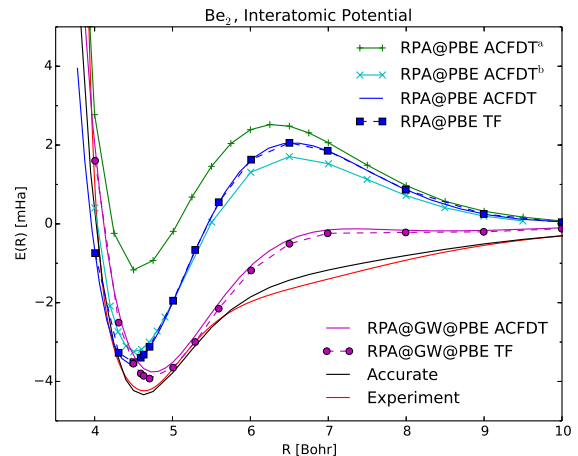

FIG. 1. Interatomic potential of Be$_2$. Red line: experiment [1]; black line: accurate CI [12]; green plus and line (a): RPA on top of PBE by ACFDT from Ref. [27]; cyan crosses and line (b): RPA on top of PBE by ACFDT from Ref. [26]; blue continuous line: RPA on top of PBE by ACFDT, our calculation; blue squares and dashed line: RPA on top of PBE by the trace formula, Eq. (4); magenta continuous line: RPA on top of GW and PBE by ACFDT; magenta circles and dashed line: RPA on top of GW and PBE by TF.

can be important. Our result is for this reason closer, surprisingly, to the one of Ref. [26] obtained by a much different implementation, plane-waves and norm-conserving pseudopotentials. Nevertheless, all RPA@PBE calculations present qualitatively the same unphysical feature, a bump at 6–7 Bohr, in contrast to the experiment and the accurate CI calculation. Note that the bump is completely absent in the original DFT PBE interatomic potential which is all over strongly attractive with a deep minimum and large binding energy (see Ref. [25]). Finally, we present curves calculated at the same level of direct RPA but using a GW corrections on top of PBE. The most important point is that there is a clear improvement in RPA@GW@PBE with respect of RPA@PBE. The bump is much reduced, though is still present. The binding energy is also improved, though still underestimated. The bonding length is now overestimated.

The bump at 6–7 Bohr seems related to the starting point, DFT PBE (but also LDA, see Ref. [26]) which our GW calculation with self-consistency on the eigenvalues is only partially able to correct. Indeed, an RPA calculation on top of HF does not present the unphysical bump, as it is evident in Fig. 2 where we report both our TF and the ACFDT of Ref. [26] RPA@HF results. Both present a correct attractive behaviour, although the original HF interatomic potential (Fig. 2) is repulsive. Nevertheless the dissociation curve is too flat (though less in our calculation), and the binding energy is severely underestimated. However, also when starting from HF, the introduction of GW corrections introduces an important improvement.
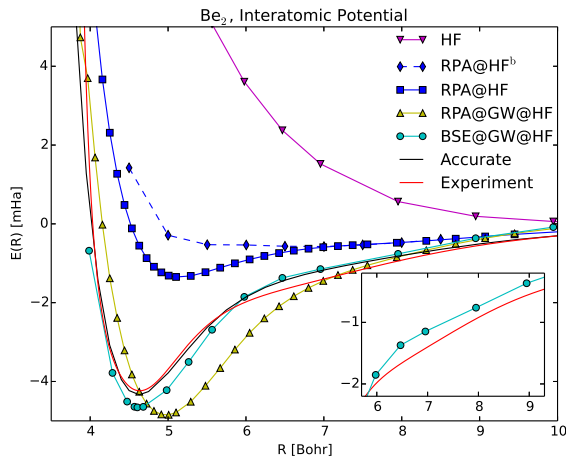
FIG. 2. Interatomic potential of Be_2. Red line: experiment [1]; black line: accurate CI [12]; magenta triangles down and line: HF; blue diamonds and dashed line: RPA on top of HF by ACFDT from Ref. [27]; blue squares and line: RPA on top of HF by TF; yellow triangles up and line: RPA on top of GW and HF; cyan circles and line: BSE on top of GW and HF by the TF formula Eq. (4).

The RPA@GW@HF curve (Fig. 2) is much closer to the accurate and experimental result, though it presents a $\sim$10% overestimation of both the binding energy and length. Finally we show the curve calculated solving the Bethe-Salpeter equation on top of a GW electronic structure and starting from HF. The result is, beyond any expectation, impressively good. The equilibrium length is within 0.02 Bohr from the exact value, and the binding energy is only 0.3 mHa overestimated. These values are even more accurate than the VMC and DMC ones [17], outperforming as well quantum chemistry methods like MP2 and even CCSD [27, 55]. Notice also that any change we have introduced to the standard procedure, like solving the BSE directly on top of HF, or considering an unscreened kernel like in TDHF, immediately destroys the good agreement, providing even much worse results in some cases. Our BSE result seems better than the most advanced ACFDT TDDFT approximations of Ref. [25], like the RPA+ and RPA+SOSEX, which are unbound, and also the RPA+rSE, which provides a good binding energy and length but still presents a bump at 6–7 Bohr. The range-separated hybrid RSH+RPAx of Ref. [27] is certainly the ACFDT TDDFT approximation closer to the physics underneath the GW+BSE approach whose path to correlations is represented by the introduction of screening. RSH+RPAx tries to mimic this physics by introducing two ranges of different screened exchange, and in Be_2 obtains a clear improvement toward the good shape without the bump, but the binding energy and length are not yet sufficient. This can only be obtained by an approach presenting continuous variation of the screening at all ranges, like in GW+BSE.

Finally, the BSE on top of the GW approximation result seems even able to reproduce an unusual feature which has been pointed out in the accurate experiment of Ref. [1]. In the Inset of Fig. 2 we show a zoom on the region [6,9] Bohr ($\sim$[3,4.5] Å) where van der Waals (vdW) interaction effects should enter into play and where in the past it was conjectured a vdW secondary (or even the only main) minimum. In this region the experiment presents an evident flattening which makes the interatomic potential deviate from the simple Morse potential, towards a more complex expanded Morse oscillator (EMO, see Ref. [1] and its Fig. 3). The EMO shape seems needed to best fit the experimental vibrational spectrum of Ref. [1] and seems a particularity of this dimer in which there is competition between covalent and vdW interactions. The latter is unable to produce even a secondary minimum, but should have an influence on the shape of the interatomic potential distorting it from the simple Morse oscillator towards a flattening. Our BSE@GW@HF curve also presents this flattening, though shifted with respect to the experiment. It is anyway impressive that we were able to describe such a delicate balance between covalent and vdW bonding which only arises from correlations. This means that BSE provides an at least qualitatively good description of high order correlation effects.

Conclusions. We have calculated the Be_2 interatomic potential along its dissociation path by an approach within *ab initio* many-body perturbation theory relying on the trace formula, as an alternative to the TDDFT ACFDT formalism. Our approach has been validated against TDDFT ACFDT calculations already in the literature. The introduction of GW corrections already provides an important improvement on the interatomic potential shape and also on the binding energy and length. At the level of BSE we got a Be_2 interatomic potential in very good agreement with the experiment and accurate CI calculations. We were even able to reproduce a flattening observed in the experiment due to a delicate balance of correlations for a competition between covalent and van der Waals bonding.

[1] J. M. Merritt, V. E. Bondybey, and M. C. Heaven, Science **324**, 1548 (2009).
[2] I. Røeggen and J. Almlöf, Int. J. Quantum Chem. **60**, 453 (1996), see Table I.
[3] G. Herzberg, Z. Phys. **57**, 601 (1929).
[4] L. Herzberg, Z. Phys. **84**, 571 (1933).
[5] J. H. Bartlett Jr. and W. H. Furry, Phys. Rev. **38**, 1615 (1931).

[6] C. F. Bender and E. R. Davidson, J. Chem. Phys. **47**, 4972 (1967).

[7] M. R. A. Blomberg and P. E. M. Siegbahn, Int. J. Quantum Chem. **14**, 583 (1978).

[8] S. Wilson, Mol. Phys. **49**, 1489 (1983).

[9] J. M. Brom Jr., W. D. Hewett Jr., and W. Weltner Jr., J. Chem. Phys. **62**, 3122 (1975).

[10] V. E. Bondybey, Chem. Phys. Lett. **109**, 436 (1984).

[11] R. J. Harrison and N. C. Handy, Chem Phys. Lett. **98**, 97 (1983).

[12] I. Røeggen and L. Veseth, Int. J. Quantum Chem. **101**, 201 (2005).

[13] R. Martin, L. Reining, and D. M. Ceperley, *Interacting Electrons* (Cambridge University Press, Cambridge, England, 2016).

[14] T. Helgaker, P. Jorgensen, and J. Olsen, *Molecular Electronic-structure Theory* (Wiley, 2008).

[15] M. Casula, C. Attaccalite, and S. Sorella, J. Chem. Phys. **121**, 7110 (2004).

[16] M. Casula, C. Filippi, and S. Sorella, Phys. Rev. Lett. **95**, 100201 (2005).

[17] M. Marchi, S. Azadi, M. Casula, and S. Sorella, J. Chem. Phys. **131**, 154116 (2009).

[18] M. Fuchs and X. Gonze, Phys. Rev. B **65**, 235109 (2002).

[19] E. Runge and E. K. U. Gross, Phys. Rev. Lett. **52**, 997 (1984).

[20] E. K. U. Gross and W. Kohn, Phys. Rev. Lett. **55**, 2850 (1985).

[21] D. C. Langreth and J. P. Perdew, Solid State Commun. **17**, 1425 (1975).

[22] D. C. Langreth and J. P. Perdew, Phys. Rev. B , 2884 (1977).

[23] F. Furche, Phys. Rev. B **64**, 195120 (2001).

[24] A. Heßelmann and A. Görling, Mol. Phys. **109**, 2473 (2011).

[25] X. Ren, P. Rinke, C. Joas, and M. Scheffler, J. Mater. Sci. **47**, 7447 (2012).

[26] H.-V. Nguyen and G. Galli, J. Chem. Phys. **132**, 044109 (2010).

[27] J. Toulouse, I. C. Gerber, G. Jansen, A. Savin, and J. G. Ángyán, Phys. Rev. Lett. **102**, 096404 (2009).

[28] L. Hedin, Phys. Rev. **139**, A796 (1965).

[29] E. E. Salpeter and H. A. Bethe, Phys. Rev. **84**, 1232 (1951).

[30] W. Hanke and L. J. Sham, Phys. Rev. Lett. **43**, 387 (1979).

[31] P. Ring and P. Schuck, *The Nuclear Many-Body Problem* (Springer, New York, 1980) see Eq. (8.93a), (8.93b) and (8.94b).

[32] D. J. Rowe, Phys. Rev. **175**, 1283 (1968), see Eq. (59).

[33] K. Sawada, Phys. Rev. **106**, 372 (1957).

[34] M. Gell-Mann and K. A. Brueckner, Phys. Rev. **106**, 364 (1957).

[35] K. Sawada, K. A. Brueckner, N. Fukuta, and R. Brout, Phys. Rev. **108**, 507 (1957).

[36] N. Fukuta, F. Iwamoto, and K. Sawada, Phys. Rev. **135**, A932 (1964), see Eq. (2.11) and previous discussion.

[37] F. Furche, J. Chem. Phys. **129**, 114105 (2008).

[38] G. E. Brown and C. W. Wong, Nucl. Phys. **A100**, 241 (1967).

[39] D. J. Rowe, Rev. Mod. Phys. **40**, 153 (1968).

[40] M. E. Casida, in *Recent Advances in Density Functional Methods. Recent Advances in Computational Chemistry*, Vol. 1, edited by D. E. Chong (World Scientific, Singapore, 1995) p. 155.

[41] M. E. Casida, in *Recent Developments and Application of Modern Density Functional Theory*, edited by J. M. Seminario (Elsevier, Amsterdam, 1996) p. 391.

[42] B. Jancovici and D. H. Schiff, Nucl. Phys. **58**, 678 (1964).

[43] More exactly $E_0^0 = \langle\Psi_0^0|\hat{H}|\Phi_0^0\rangle$ where Ψ_0^0 is the ground-state killed by the boson operators, $\hat{C}_t|\Psi_0^0\rangle = 0$. Since $\hat{C}_t \simeq \hat{c}_p^\dagger\hat{c}_h$, the 0-order ground state Φ_0, killed by the $\hat{c}_p^\dagger\hat{c}_h|\Phi_0\rangle = 0$, is an approximation for Ψ_0^0, and $\hat{C}_t|\Phi_0\rangle \simeq 0$ is approximated to zero.

[44] T. Olsen and K. S. Thygesen, J. Chem. Phys. **140**, 164116 (2014).

[45] C. Holzer, X. Gui, M. E. Harding, G. Kresse, T. Helgaker, and W. Klopper, J. Chem. Phys. **149**, 144106 (2018).

[46] T. H. Dunning, J. Chem. Phys. **90**, 1007 (1989).

[47] C. Hattig, Phys. Chem. Chem. Phys. **7**, 59 (2005).

[48] M. Valiev, E. Bylaska, N. Govind, K. Kowalski, T. Straatsma, H. V. Dam, D. Wang, J. Nieplocha, E. Apra, T. Windus, and W. de Jong, Comput. Phys. Commun. **181**, 1477 (2010).

[49] D. Jacquemin, I. Duchemin, and X. Blase, J. Chem. Theory Comput. **11**, 3290 (2015).

[50] I. Duchemin, C. A. Guido, D. Jacquemin, and X. Blase, Chem. Sci. **9**, 4430 (2018).

[51] X. Gui, C. Holzer, and W. Klopper, J. Chem. Theory Comput. **14**, 2127 (2018).

[52] J. P. Perdew, K. Burke, and M. Ernzerhof, Phys. Rev. Lett. **77**, 3865 (1996).

[53] X. W. Sheng, L. Mentel, O. V. Gritsenko, and E. J. Baerends, J. Comput. Chem. **32**, 2896 (2011).

[54] M. Mentel and E. J. Baerends, J. Chem. Theory Comput. **10**, 252 (2014).

[55] V. F. Lotrich, R. J. Bartlett, and I. Grabowski, Chem. Phys. Lett. **405**, 43 (2005).